Howard Hughes Medical Institute

Published as: *Science*. 2009 April 17; 324(5925): 354–359.

Optical Deconstruction of Parkinsonian Neural Circuitry

Viviana Gradinaru[1,2,*], **Murtaza Mogri**[1,*], **Kimberly R. Thompson**[1], **Jaimie M. Henderson**[3], **Karl Deisseroth**[1,4,†]

[1]Department of Bioengineering, Stanford University, Stanford, CA 94305, USA.

[2]Program in Neuroscience, Stanford University, Stanford, CA 94305, USA.

[3]Department of Neurosurgery, Stanford University, Stanford, CA 94305, USA.

[4]Department of Psychiatry and Behavioral Sciences, Stanford University, Stanford, CA 94305, USA.

Abstract

Deep brain stimulation (DBS) is a therapeutic option for intractable neurological and psychiatric disorders, including Parkinson's disease and major depression. Because of the heterogeneity of brain tissues where electrodes are placed, it has been challenging to elucidate the relevant target cell types or underlying mechanisms of DBS. We used optogenetics and solid-state optics to systematically drive or inhibit an array of distinct circuit elements in freely moving parkinsonian rodents and found that therapeutic effects within the subthalamic nucleus can be accounted for by direct selective stimulation of afferent axons projecting to this region. In addition to providing insight into DBS mechanisms, these results demonstrate an optical approach for dissection of disease circuitry and define the technological toolbox needed for systematic deconstruction of disease circuits by selectively controlling individual components.

Parkinson's disease (PD) is a debilitating neurodegenerative disorder resulting from the loss of dopaminergic (DA) neurons in the substantia nigra pars compacta (SNc), leading to abnormal neuronal activity in the basal ganglia (BG). DA depletion in the BG leads to altered activity of the subthalamic nucleus (STN) and globus pallidus pars interna (GPi), which has been linked to clinical deficits in movement initiation and execution (1–3). On the basis of these observations from animal models and the fact that lesions of the BG can be therapeutic in PD, high-frequency (>90 Hz) stimulation (HFS) of the STN (deep brain stimulation or DBS) has emerged as a highly effective treatment for medically refractory PD (4–6).

Exactly how DBS exerts its therapeutic effects is a matter of controversy (7–10) for three major reasons. First, because of the heterogeneity of brain tissue (11), it is unclear which circuit elements are responsible for the therapeutic effects. Second, HFS is intrinsically a complicated manipulation because target neurons can respond with increased, decreased, or

[†]To whom correspondence should be addressed. deissero@stanford.edu.
[*]These authors contributed equally to this work.

Supporting Online Material
www.sciencemag.org/cgi/content/full/1167093/DC1

mixed temporal patterns of activity; as a result, the magnitude and even the sign of target cell responses to DBS are unknown. Finally, it is difficult to assess the net outcome of DBS on overall activity in the target cells and region, because electrical stimulation creates artifacts that prevent direct observation of local circuit responses during HFS itself. Together, these challenges point to the need to understand, to improve, and to generalize (12–15) this important treatment modality.

We have developed and employed optogenetics technology based on single-component microbial light-activated regulators of transmembrane conductance and fiber optic– and laser diode–based in vivo light delivery (16–24). The channelrhodopsins, including VChR1 (24) and ChR2 (19), encode light-activated cation channels that can be expressed in neurons under cell type–specific promoters. In contrast, the halorhodopsins (e.g., NpHR) are light-activated Cl^- pumps, and NpHR-expressing neurons are hyperpolarized and inhibited from firing action potentials when exposed to 590-nm light in intact neural tissue (20, 21). The ChR2–NpHR system is ideally suited to dissect PD circuitry because of three features that map well onto the challenges outlined above. First, optogenetics allows genetically targeted photosensitization of individual circuit components within the STN area and, therefore, testing of hypotheses regarding the causal role of individual cell types. Second, inhibition or excitation of target cells by direct hyperpolarization or depolarization can be achieved, which reduces complications such as soma-axon decoupling (25, 26), in which cell bodies can be inhibited and axons stimulated by HFS. Third, optogenetics allows simultaneous optical control and electrophysiological recording of local neuronal activity in vivo with integrated fiber-electrode “optrodes” (27) and avoids electrical stimulus artifacts, which may mask crucial neural responses.

In all of this, optogenetics maintains the millisecond temporal precision of electrodes. Therefore, optogenetics, in principle, could be used to systematically probe specific circuit elements with defined frequencies of true excitation or inhibition in freely behaving parkinsonian rodents.

Optical inhibition of STN.

To first address the most widely held hypothesis in the field, we asked if direct, reversible, bona fide inhibition of local-circuit excitatory STN neurons would be therapeutic in PD. The STN measures <1 mm^3 in rats (28), but targeting accuracy can be aided by extracellular recordings during opsin vector introduction, because STN is characterized by a particular firing pattern that is distinguishable from bordering regions (Fig. 1A and fig. S1C) (29).

The STN is a predominantly excitatory structure (30) embedded within an inhibitory network. This anatomical arrangement enables a targeting strategy for selective STN inhibition (Fig. 1B), in which enhanced NpHR (eNpHR) (21) is expressed under control of the calcium/calmodulin-dependent protein kinase IIα (CaMKIIα) promoter, which is selective for excitatory glutamatergic neurons and not inhibitory cells, fibers of passage, glia, or neighboring structures (18). In this way, true optical inhibition is targeted to the dominant local neuron type within STN.

Optical circuit interventions were tested in rats that had been made hemiparkinsonian by injection of 6-hydroxydopamine (6-OHDA) unilaterally into the right medial forebrain bundle (MFB). Loss of nigral dopaminergic cells after 6-OHDA administration was confirmed by decreased tyrosine hydroxylase levels unilaterally in the SNc (fig. S1A). These hemiparkinsonian rodents have specific deficits in contralateral (left) limb use and display (rightward) rotations ipsilateral to the lesion, which increase in frequency when the subjects are given amphetamine to facilitate functional evaluation and decrease in frequency on treatment with dopamine agonists (31) or after electrical DBS (Fig. 1D, right). This amphetamine-induced rotation test is widely used for identifying treatments in hemi-parkinsonian rodents and can be complemented with other behavioral assays such as locomotion, climbing, and head position bias. To inhibit the excitatory STN neurons directly, we delivered lentiviruses carrying eNpHR under the CaMKIIα promoter to the right STN of the hemiparkinsonian rats. CaMKIIα::eNpHR labeled with enhanced yellow fluorescent protein (EYFP) expression was specific to excitatory neurons (as shown by CaMKIIα and glutamate expression; Fig. 1B, right; and fig. S2A), robust (95.73% ± 1.96% SEM infection rate assessed in $n = 220$ CaMKIIα-positive cells), and restricted to the STN (Fig. 1B, left and middle). To validate the resulting physiological effects of optical control, a hybrid optical stimulation–electrical recording device (optrode) was used in isoflurane-anesthetized animals to confirm that eNpHR was functional in vivo, potently inhibiting (>80%) spiking of recorded neurons in the STN (Fig. 1C; fig. S4, A and B; and fig S5A). This cell type–targeted inhibition was temporally precise and reversible, and it extended across all frequency bands of neuronal firing (Fig. 1C and fig. S7A).

For behavioral rotation assays in the hemi-parkinsonian rats, the STN-targeted fiber optic was coupled to a 561-nm laser diode to drive eNpHR. Electrical DBS was highly effective in reducing pathological rotational behavior, but despite precise targeting and robust physiological efficacy of eNpHR inhibition, the hemiparkinsonian animals did not show even minimal changes in rotational behavior with direct true optical inhibition of the local excitatory STN neurons (Fig. 1D). In addition, there was no effect on path length and head position bias in response to light during these experiments (29). Although muscimol and lidocaine administration to the region of the STN in monkeys and rodents can relieve parkinsonian symptoms (32), the data in Fig. 1 show that the more restricted intervention of selectively decreasing activity in excitatory local neurons of the STN appeared not to be sufficient by itself to affect motor symptoms.

Another possibility is that DBS could be driving secretion of glial modulators that would have the capability to modulate local STN circuitry; this would be consistent with recent findings (33) indicating that a glial-derived factor (adenosine) accumulates during DBS and plays a role in DBS-mediated attenuation of thalamic tremor. Indeed, the STN expresses receptors for glia-derived modulators (34), which can inhibit postsynaptic currents in the STN (35). ChR2 presents an interesting possibility for recruitment of glia; when opened by light, in addition to Na^+ and K^+ ions, ChR2 can also pass trace Ca^{2+} currents (36, 37) that trigger Ca^{2+} waves in and activate ChR2-expressing astroglia (38). We used a glial fibrillary acidic protein (GFAP) promoter to target ChR2 to local astroglia, validated with GFAP and S100β staining (Fig. 2A and fig. S2B, respectively). Optrode recordings revealed that blue light stimulation of STN following transduction with GFAP::ChR2 reversibly inhibited

neuronal firing in the STN (Fig. 2B and fig. S3A), with variable delay on a time scale of seconds. However, recruiting astroglial cells by this mechanism was not sufficient to cause even trace responses in motor pathology in parkinsonian rodents (Fig. 2C and fig. S3B). Path length and head position bias were also not affected by light during these experiments (29). Although these data do not exclude the importance of local STN inhibition as a contributing factor in DBS response, as not all STN neurons may be affected in the same way by indirect glial modulation and, as in Fig. 1, breakthrough activity could occur, the direct activation of local glial cells appeared not to be sufficient to treat parkinsonian symptoms, pointing to consideration of other circuit mechanisms.

Optogenetic excitation of targeted STN cells.

Network oscillations at particular frequencies could play important roles in both PD pathology and treatment. For example, PD is characterized by pathological levels of beta oscillations in the basal ganglia, and synchronizing STN at gamma frequencies may ameliorate PD symptoms, whereas beta frequencies may worsen symptoms (39, 40). Because simple inhibition of excitatory cell bodies in the STN did not affect behavioral pathology and because HFS (90 to 130 Hz) is used for electrical DBS, we used ChR2 to drive high-frequency oscillations in this range within the STN. We injected CaMKIIα::ChR2 into the STN (Fig. 3A) and used pulsed illumination with a 473-nm laser diode to activate excitatory neurons in the STN (Fig. 3B and fig. S5B), during behavioral testing in parkinsonian rodents (Fig. 3C and fig. S3C). Despite robust effects on the high-frequency power of neuronal spike rate in STN of anesthetized animals (fig. S7B), HFS delivered locally to the STN area failed to affect PD behavioral symptoms (path length and head position bias were unchanged by light) (29). Animals tested in parallel with beta frequency pulses also showed no behavioral response, indicating that (although not excluding a contributory role) directly generated oscillations within the STN excitatory neurons are not sufficient to account for therapeutic effects.

Measuring the volume of tissue recruited in STN.

We have previously measured in cortical and hypothalamic tissue the propagation of blue light in the setting of laser diode–fiber optic illumination; we observed that substantial tissue volumes (comparable to that of the STN) could reliably be recruited at a light-power density sufficient to drive physiologically significant microbial opsin currents (17, 18). It was important to repeat and extend these measurements to the PD setting. First, we confirmed that the propagation measurements of blue light (473 nm) in brain tissue represent a lower bound on the volume of tissue recruited, owing to reduced scattering of lower-energy photons delivered from the 561-nm laser diode; therefore, sufficient light power is present to activate opsins within 1.5 mm of the fiber for either wavelength of light (Fig. 4A). We next extended these findings with a functional assay for tissue recruitment under conditions mimicking our behavioral experiments (Fig. 4, B and C). After an in vivo optical stimulation paradigm targeted to the CaMKIIα::ChR2–expressing STN in freely moving rats, we performed immunohisto-chemistry for c-fos, a biochemical marker of neuronal activation. We observed robust c-fos activation in STN (Fig. 4B) over a widespread volume (Fig. 4C); indeed, as expected from our light-scattering measurements and tissue geometry, we found

that at least 0.7 mm^3 of STN is recruited by light stimulation, which closely matched the actual volume of the STN (Fig. 4C). Therefore, light penetration was not limiting because the entire STN is recruited by the optical modulation paradigms of Figs. 1 to 3.

Optical control of afferent axons in STN.

Therapeutic effects could arise from driving axonal projections that enter the STN, as DBS electrodes will potently modulate not just local cells and their efferents, but also afferent fibers. Optogenetics discriminates between these two possibilities, as the lentiviruses transduce somata without transducing afferent axons (27). To assess the possibility that PD motor behavioral responses are modulated by targeting afferent projections to the STN, we used Thy1::ChR2 transgenic mice (22, 23) in which ChR2 is expressed in projection neurons, and we verified that in Thy1::ChR2 line 18, ChR2-YFP is excluded from cell bodies in the STN but is abundant in afferent fibers (Fig. 5A).

We conducted optrode recordings in anesthetized 6-OHDA mice (fig. S1B) (41, 42) to assess local effects on STN physiology of driving afferent axons selectively and found frequency-dependent effects (Fig. 5B). First, we observed that HFS of afferent fibers to the STN potently reduced STN spiking across all frequency bands; this effect did not completely shut down local circuitry, as low-amplitude high-frequency oscillations persisted during stimulation (Fig. 5B; fig. S4, C and D; and fig. S5C). Next, we found that LFS of afferent fibers increased beta-frequency firing in the STN without affecting endogenous bursting (Fig. 5B, fig. S5D, and fig. S7E). We next assessed the impact of these specific interventions on PD behavior in 6-OHDA mice, and for the first time among the optogenetic interventions, we observed marked effects. Driving STN afferent fibers with HFS robustly and reversibly ameliorated PD symptoms, measured by rotational behavior and head position bias (Fig. 5C). The HFS effects were not subtle; indeed, in nearly every case these severely parkinsonian animals were restored to behavior indistinguishable from normal, and in every case, the therapeutic effect immediately and fully reversed, with return of ipsilateral rotations upon discontinuation of the light pulse paradigm. Notably, treated animals could freely switch directions of movement and head position from left to right and vice versa. In striking contrast with optical HFS, optical LFS (20 Hz) of the same afferent fibers worsened PD symptoms by driving increased ipsilateral rotational behavior (Fig. 5C), which demonstrated that the behavioral effects seen do not result simply from driving unilateral activity. Therefore, in contrast to direct STN cellular interventions, driving STN afferent fibers with HFS and LFS differentially modulated PD symptoms in a manner corresponding to frequencies of stimulation linked clinically to ameliorated or exacerbated PD symptoms.

Optical control of layer V motor cortex projection neurons.

A diverse array of fibers from widespread brain areas converge on the STN, which may underlie the utility of the STN as a focal DBS target. Many of these afferents likely contribute together to the therapeutic effects, and it is unlikely that a single source of fibers completely accounts for the behavioral effects seen. However, we explored these afferents in greater detail to determine the general class of fibers that may be contributory.

Thy1::ChR2 animals display ChR2 expression chiefly in excitatory projection neurons (22, 23). Indeed, the inhibitory markers glutamic acid decarboxylase isoform 67 (GAD67) and γ-aminobutyric acid (GABA) were not detectable in Thy1::ChR2 fibers within STN (Fig. 6A, left), which effectively ruled out contributions from the GABAergic pallidal projections (LGP–GPe). We also found no localization of major neuromodulatory markers (dopamine and acetylcholine) within the STN Thy1::ChR2 fibers (fig. S2C), which ruled out dopaminergic substantia nigra pars reticulata as a relevant fiber origin as well. We next explored possible sources of excitatory fibers and found no expression of ChR2-YFP in the cell bodies of the excitatory parafascicular or pedunculopontine nuclei, potential contributors of excitatory fibers to the STN. Within neocortex of these mice, however, ChR2-YFP is expressed strongly in excitatory neurons that project to STN (22, 23). Because pathologically strong connectivity between STN and primary motor cortex M1 has been suggested to underlie PD circuit dysfunction (43, 44), we therefore explored M1 as a possible contributor.

We verified in Thy1::ChR2 M1 the presence of strong and selective ChR2 expression largely restricted to layer V neurons and corresponding apical dendrites (22, 23) but not in cells within other layers (Fig. 6A, right). To probe the functional connectivity between these layer V projection neurons and STN in the PD animals, we conducted a separated-optrode experiment in anesthetized animals in which the fiber-optic and recording electrodes were placed in two different brain regions in Thy1::ChR2 animals (Fig. 6B). By driving M1 layer V projection neurons and simultaneously recording in both M1 and STN, we found that precise M1 stimulation of this kind potently influenced neural activity in the STN (Fig. 6C and fig. S7, C and D) and that M1 layer V neurons could be antidromically recruited by optical stimulation in the STN (fig. S6). Whereas, as noted above, many local afferents in the STN region, including those from the ZI, are likely to underlie the complex therapeutic effects of DBS, functional influences between M1 layer V and STN could be significant contributors. Indeed, we found that selective M1 layer V HFS optical stimulation sufficed to ameliorate PD symptoms in a manner similar to that of STN stimulation in an array of measures ranging from rotational behavior (Fig. 6D) to head position bias and locomotion (Fig. 6, E and F). As with STN stimulation, pathological rotations and head position bias were reduced by optical HFS to M1; in contrast, without augmenting the pathology, optical 20 Hz (LFS) stimulation to M1 had no therapeutic effect (Fig. 6, D, E, and F), and even at the highest light intensities achievable without epilepto-genesis, M1 LFS did not drive or modify rotational behavior, unlike M2 LFS cortical stimulation that can elicit contralateral rotations (27). Finally, increased functional mobility with M1 HFS but not LFS was confirmed with quantification of increased distance and speed of locomotion in PD Thy1::ChR2 mice; in the absence of amphetamine, M1 HFS allowed the otherwise bradykinetic animals to move freely without eliciting rotational behavior (Fig. 6F).

Discussion.

A major promise of optogenetics has been the potential for dissection of disease circuitry and treatment mechanisms. Here, we demonstrate that this potential can be realized. Systematically targeting different elements of the disease circuit, we implicate direct

frequency-dependent effects on afferents to the STN region as a major direct target of deep brain stimulation in PD.

Cortical-STN interactions have been previously considered in PD; indeed, motor cortex activity may be elevated in PD and reduced in PD treatment (45, 46), and abnormal oscillatory activity may occur between the cortex and the basal ganglia in PD patients during movement (32, 47, 48). Cortical stimulation could restore balance to parkinsonian circuitry that is overly devoted to one kind of activity to the exclusion of others (44), either by disrupting the pathological activity pattern (e.g., low-frequency bursting), by promoting through-put of patterns encoding motor behaviors oppositional or compensatory to the lesion pathology, or both. Cortical stimulation in human beings has been a subject of interest and controversy (49), with some studies showing promising results for PD treatment (50–55) and others less supportive (56–58). Our data, in implicating deep layer V neurons as sufficient targets in primary motor cortex, may help address these issues by informing the design of cortical interventions with regard to subdural rather than superficial extradural stimulation. Even with subdural stimulation, optimal cortical stimulation in patients will certainly face particular challenges because of broad cortical representation, and identifying the cortical subregion most functionally connected to STN will be important. Clinical translation of these concepts will benefit from ongoing work in animal models to facilitate rapid mapping of stimulus space for identification of optimal duty cycles (percentage of time pulse is on during stimulation) and pulse patterns.

It is important to note that these findings do not exclude other important contributions to DBS targets or disease symptoms. Not only are other afferents to the STN potential upstream factors in STN-initiated therapeutic effects, but all STN-initiated effects will be implemented downstream through the interconnected basal ganglia, cortical, brainstem, and thalamic motor pathways, with many potential nodes for intervention. Both the disease and treatment are extraordinarily complex; the fact that DBS can improve many PD symptoms, including tremor, rigidity, and bradykinesia—but not others, such as speech impairment, depression, and dementia—points to the need for ongoing work to map and functionally interrogate disease circuitry beyond the brain regions investigated here. DBS can also encounter limitations as a therapy even for the symptoms that typically respond. These issues may be linked to cell type– specific responses and suggest that disease model investigations will be greatly facilitated by the optogenetic approach.

Axon tract modulation with high temporal precision could turn out to be a common theme in DBS (12–15, 26), as these collections of fibers represent compact nodes for accessing activity converging from a broader area. Even without detailed knowledge of the relevant neural code, simple alterations in the propagation of activity through white matter tracts or disrupting circuit loops could represent final common pathways for disease and treatment (59). However, for PD as well as for other neurological and psychiatric diseases, maintaining high temporal precision of the circuit interrogation technology will be crucial, because as illustrated here, fundamentally different effects are seen when driving the same cell type at different temporal frequencies. Indeed, themes of synchrony and oscillations driven by particular cell and fiber types will likely be common to other brain stimulation–responsive

diseases, such as depression and epilepsy, and will underscore the importance of understanding and generalizing DBS.

Supplementary Material

Refer to Web version on PubMed Central for supplementary material.

Acknowledgments

60. K.D. is supported by the Kinetics Foundation, the William M. Keck Foundation, the Snyder Foundation, the Albert Yu and Mary Bechmann Foundation, and the Wallace Coulter Foundation, as well as by California Institute for Regenerative Medicine, the McKnight Foundation, the Esther A. and Joseph Klingenstein Fund, NSF, National Institute of Mental Health, National Institute on Drug Abuse, and the NIH Pioneer Award. V.G. is supported by SGF and SIGF (Stanford Graduate Fellowships). M.M is supported by Bio-X and SGF Fellowships. K.R.T. is supported by NARSAD. J.M.H is supported by the Coulter Foundation, the John Blume Foundation and the Davis Phinney Foundation. We especially thank A. M. Aravanis for mentoring and advice on animal surgery and in vivo recordings, F. Zhang and H. C. Tsai for assistance with Cre-dependent opsin targeting, L. Meltzer for useful discussion, advice and help on immunohistochemistry,G. Feng and G. Augustine for collaboration on generation of the Thy-1 mice (available at the Jackson Laboratory), and V. Sohal for help with power spectra analysis. We also thank the entire Deisseroth lab for useful discussions. The materials and methods described herein are freely distributed and supported by the authors (www.stanford.edu/group/dlab).

References and Notes

1. Albin RL, Young AB, Penney JB, Trends Neurosci 12, 366 (1989). [PubMed: 2479133]
2. Alexander GE, Crutcher MD, Trends Neurosci 13, 266 (1990). [PubMed: 1695401]
3. DeLong MR, Trends Neurosci 13, 281 (1990). [PubMed: 1695404]
4. Benabid AL et al., Stereotact. Funct. Neurosurg 62, 76 (1994). [PubMed: 7631092]
5. Limousin P et al., Lancet 345, 91 (1995). [PubMed: 7815888]
6. Rezai AR et al., Neurosurgery 62 (suppl. 2), 809 (2008). [PubMed: 18596424]
7. Dostrovsky JO, Lozano AM, Mov. Disord 17, (Suppl. 3), S63 (2002).
8. Liu Y, Postupna N, Falkenberg J, Anderson ME, Neurosci. Biobehav. Rev 32, 343 (2008). [PubMed: 17187859]
9. McIntyre CC, Savasta M, Kerkerian-Le Goff L, Vitek JL, Clin. Neurophysiol 115, 1239 (2004). [PubMed: 15134690]
10. Vitek JL, Mov. Disord 17, (Suppl. 3), S69 (2002). [PubMed: 11948757]
11. Gross RE, Rolston JD, Clin. Neurophysiol 119, 1947 (2008). [PubMed: 18632306]
12. Lozano AM et al., Biol. Psychiatry 64, 461 (2008). [PubMed: 18639234]
13. Mayberg HS et al., Neuron 45, 651 (2005). [PubMed: 15748841]
14. McNeely HE, Mayberg HS, Lozano AM, Kennedy SH, J. Nerv. Ment. Dis 196, 405 (2008). [PubMed: 18477883]
15. Ressler KJ, Mayberg HS, Nat. Neurosci 10, 1116 (2007). [PubMed: 17726478]
16. Zhang F, Aravanis AM, Adamantidis A, de Lecea L,Deisseroth K, Nat. Rev. Neurosci 8, 577 (2007). [PubMed: 17643087]
17. Adamantidis AR, Zhang F, Aravanis AM,Deisseroth K, de Lecea L, Nature 450, 420 (2007). [PubMed: 17943086]
18. Aravanis AM et al., J. Neural Eng 4, S143 (2007). [PubMed: 17873414]
19. Boyden ES, Zhang F, Bamberg E, Nagel G,Deisseroth K, Nat. Neurosci 8, 1263 (2005). [PubMed: 16116447]
20. Zhang F et al., Nature 446, 633 (2007). [PubMed: 17410168]
21. Gradinaru V, Thompson KR, Deisseroth K, Brain Cell Biol 36, 129 (2008). [PubMed: 18677566]
22. Arenkiel BR et al., Neuron 54, 205 (2007). [PubMed: 17442243]
23. Wang H et al., Proc. Natl. Acad. Sci. U.S.A 104, 8143 (2007). [PubMed: 17483470]

24. Zhang F et al., Nat. Neurosci 11, 631 (2008). [PubMed: 18432196]
25. McIntyre CC, Grill WM, J. Neurophysiol 88, 1592 (2002). [PubMed: 12364490]
26. McIntyre CC, Grill WM, Sherman DL, Thakor NV, J. Neurophysiol 91, 1457 (2004). [PubMed: 14668299]
27. Gradinaru V et al., J. Neurosci 27, 14231 (2007). [PubMed: 18160630]
28. Hamani C, Saint-Cyr JA, Fraser J, Kaplitt M,Lozano AM, Brain 127, 4 (2004). [PubMed: 14607789]
29. Materials and methods are available as supporting material on Science Online.
30. Smith Y, Parent A, Brain Res 453, 353 (1988). [PubMed: 2900056]
31. Metz GA, Tse A, Ballermann M, Smith LK, Fouad K, Eur. J. Neurosci 22, 735 (2005). [PubMed: 16101755]
32. Levy R et al., Brain 124, 2105 (2001). [PubMed: 11571226]
33. Bekar L et al., Nat. Med 14, 75 (2008). [PubMed: 18157140]
34. Rivkees SA, Price SL, Zhou FC, Brain Res 677, 193 (1995). [PubMed: 7552243]
35. Shen KZ, Johnson SW, Neuroscience 116, 99 (2003). [PubMed: 12535943]
36. Zhang YP, Oertner TG, Nat. Methods 4, 139 (2007). [PubMed: 17195846]
37. Nagel G et al., Proc. Natl. Acad. Sci. U.S.A 100, 13940 (2003). [PubMed: 14615590]
38. Wang LP, Deisseroth K, unpublished observations.
39. Bronte-Stewart H et al., Exp. Neurol 215, 20 (2009). [PubMed: 18929561]
40. Wingeier B et al., Exp. Neurol 197, 244 (2006). [PubMed: 16289053]
41. Tabar V et al., Nat. Med 14, 379 (2008). [PubMed: 18376409]
42. Matsuya T et al., J. Pharmacol. Sci 103, 329 (2007). [PubMed: 17341841]
43. Li S et al., J. Neurophysiol 98, 3525 (2007). [PubMed: 17928554]
44. Degos B, Deniau JM, Le Cam J, Mailly P, Maurice N, Eur. J. Neurosci 27, 2599 (2008). [PubMed: 18547246]
45. Ridding MC, Inzelberg R, Rothwell JC, Ann. Neurol 37, 181 (1995). [PubMed: 7847860]
46. Payoux P et al., Arch. Neurol 61, 1307 (2004). [PubMed: 15313852]
47. Brown P et al., J. Neurosci 21, 1033 (2001). [PubMed: 11157088]
48. Kringelbach ML, Jenkinson N, Owen SL, Aziz TZ, Nat. Rev. Neurosci 8, 623 (2007). [PubMed: 17637800]
49. Fregni F, Simon DK, Wu A, Pascual-Leone A,J. Neurol. Neurosurg. Psychiatry 76, 1614 (2005). [PubMed: 16291882]
50. Canavero S, Paolotti R, Mov. Disord 15, 169 (2000). [PubMed: 10634262]
51. Canavero S et al., J. Neurosurg 97, 1208 (2002). [PubMed: 12450046]
52. Pagni CA, Zeme S, Zenga F, J. Neurosurg. Sci 47, 189 (2003). [PubMed: 14978472]
53. Lefaucheur JP et al., Clin. Neurophysiol 115, 2530 (2004). [PubMed: 15465443]
54. Drouot X et al., Neuron 44, 769 (2004). [PubMed: 15572109]
55. Khedr EM, Rothwell JC, Shawky OA, Ahmed MA,Hamdy A, Mov. Disord 21, 2201 (2006). [PubMed: 17219616]
56. Cilia R et al., Mov. Disord 22, 111 (2007). [PubMed: 17083104]
57. Strafella AP et al., Mov. Disord 22, 2113 (2007). [PubMed: 17894326]
58. Arle JE et al., J. Neurosurg 109, 133 (2008). [PubMed: 18590444]
59. Airan RD et al., Science 317, 819 (2007). [PubMed: 17615305]

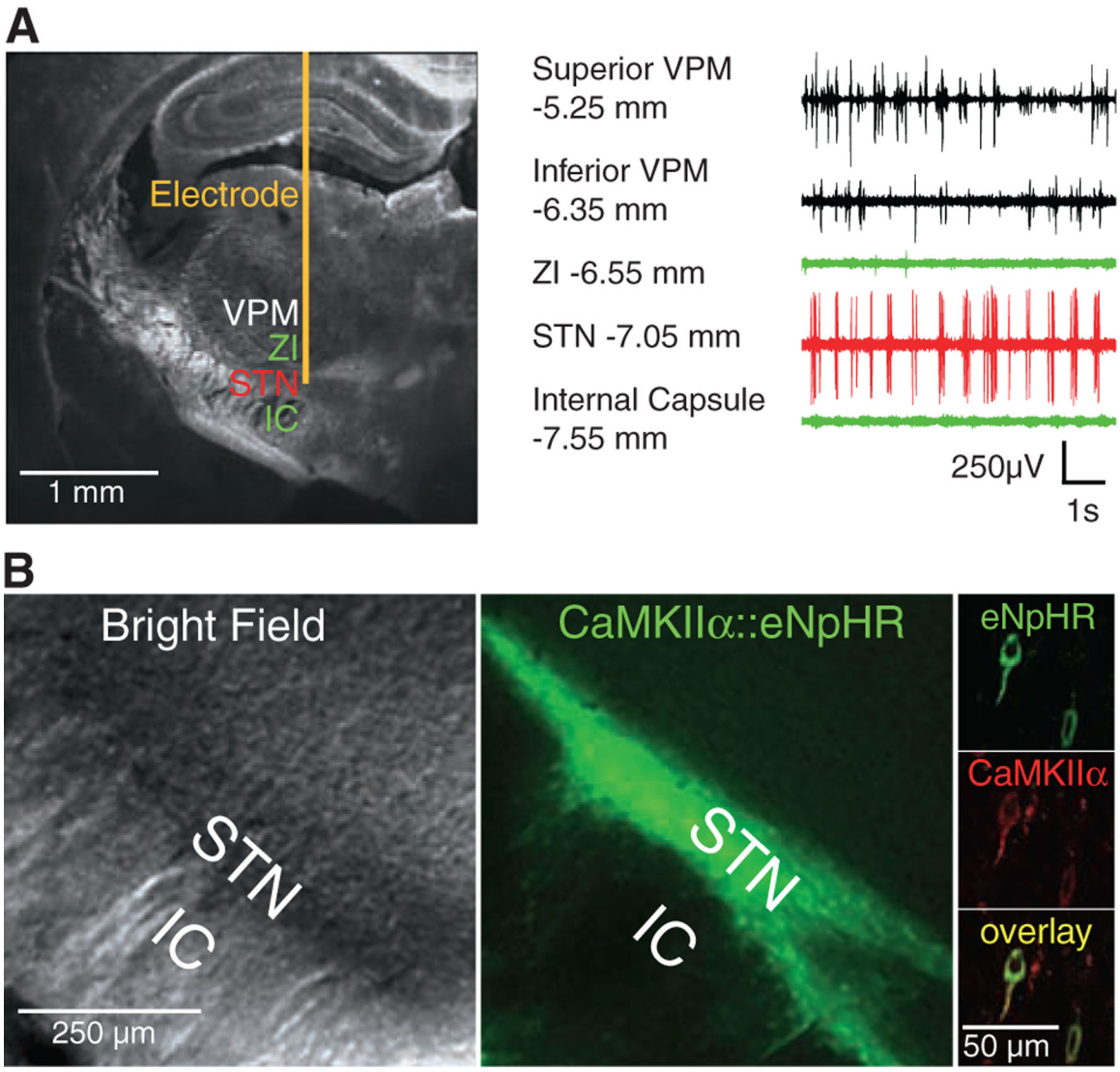

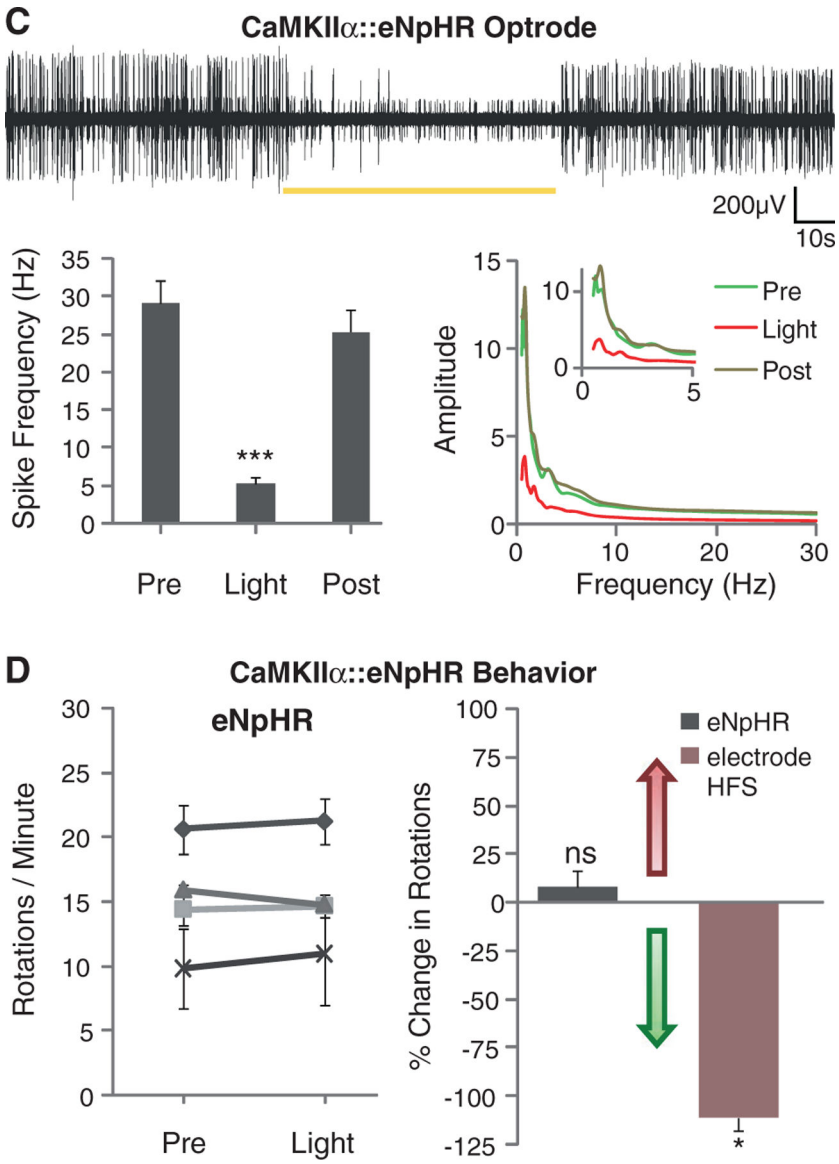

Fig. 1.

Direct optical inhibition of local STN neurons. (**A**) Cannula placement, virus injection, and fiber depth were guided by recordings of the STN, which is surrounded by the silent zona incerta (ZI) and internal capsule (IC). (**B**) Confocal images of STN neurons expressing CaMKIIα::eNpHR-EYFP and labeled for excitatory neuron-specific CaMKIIα (right). (**C**) Continuous 561-nm illumination of the STN expressing CaMKIIα::eNpHR-EYFP in anesthetized 6-OHDA rats reduced STN activity; representative optrode trace and amplitude spectrum are shown. Mean spiking frequency was reduced from 29 ± 3 to 5 ± 1 Hz (means ± SEM, $P < 0.001$, Student's t test, n = eight traces from different STN coordinates in two animals). (**D**) Amphetamine-induced rotations were not affected by stimulation of the STN in these animals ($P > 0.05$, $n = 4$ rats, t test with $\mu = 0$). The red arrow indicates direction of pathologic effects; the green arrow indicates direction of therapeutic effects. The electrical control implanted with a stimulation electrode showed therapeutic effects with HFS (120 to

130 Hz, 60-μs pulse width, 130 to 200 μA, $P < 0.05$, t test with $\mu = 0$). Percentage change of −100% indicates that the rodent is fully corrected. Data in all figures are means ± SEM ns, $P > 0.05$; *$P < 0.05$; **$P < 0.01$; and ***$P < 0.001$.

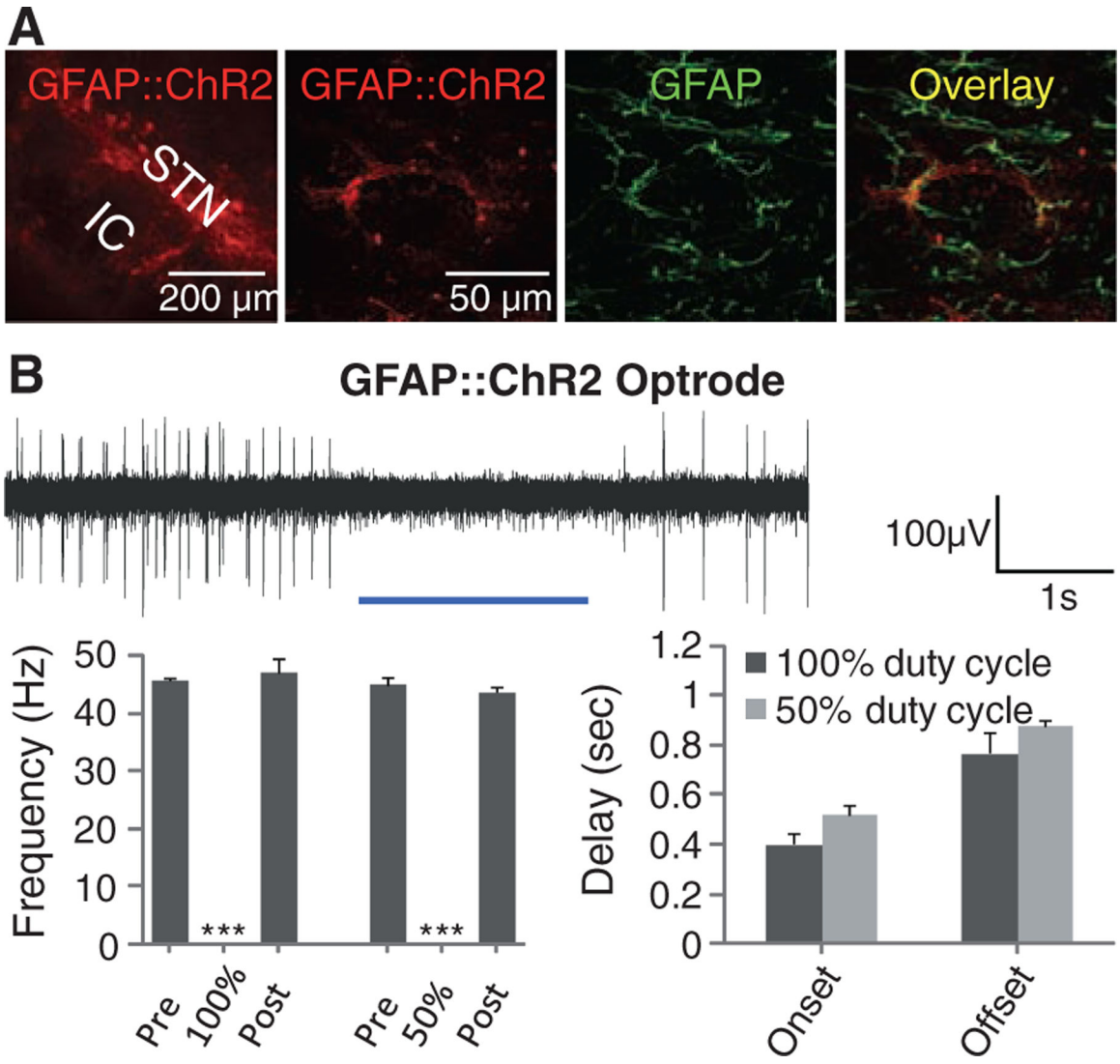

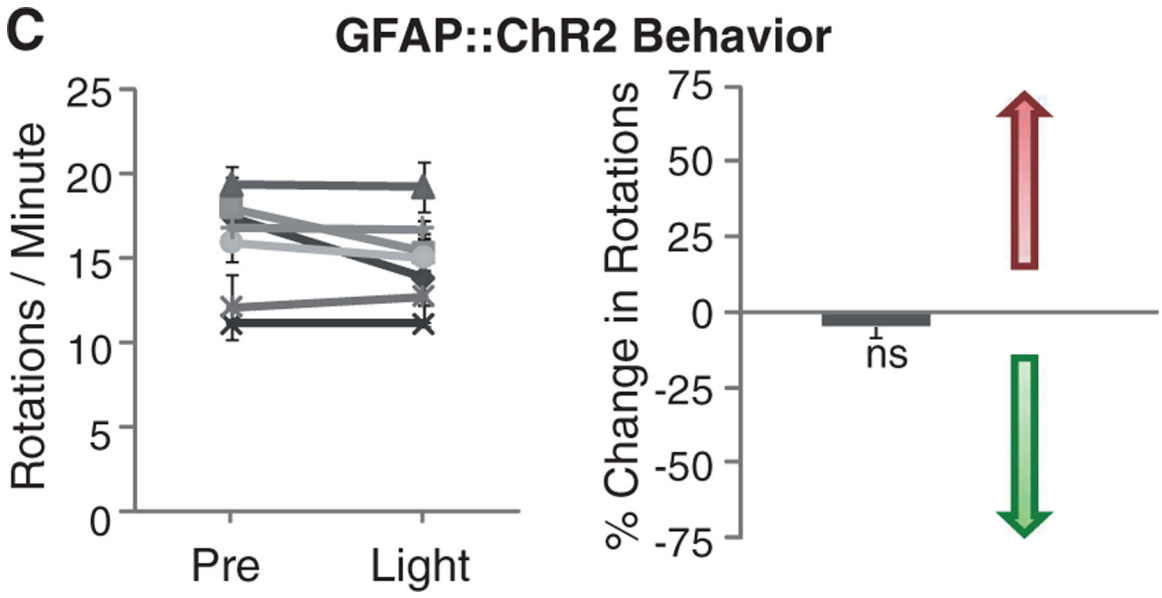

Fig. 2.

Targeting astroglia within the STN. (**A**) Confocal images show STN astrocytes expressing GFAP::ChR2-mCherry,costainedwithGFAP (right). (**B**) A 473-nm illumination of the STN expressing GFAP::ChR2-mCherry inanesthetized6-OHDA rats. Optrode recording revealed that continuous illumination inhibited STN activity with delay to onset of 404 ± 39 ms and delay to offset of 770 ± 82 ms (*n* = five traces from different STN coordinates in two animals), nevertheless, the 50% duty cycle also inhibited spiking, with delay to onset of 520 ± 40 ms and delay to offset of 880 ± 29 ms (*n* = three traces from different STN coordinates in two animals) with $P < 0.001$. (**C**) Amphetamine-induced rotations were not affected by 50% duty cycle illumination in these animals (right, $P > 0.05$, *n* = seven rats, *t* test with $\mu = 0$).

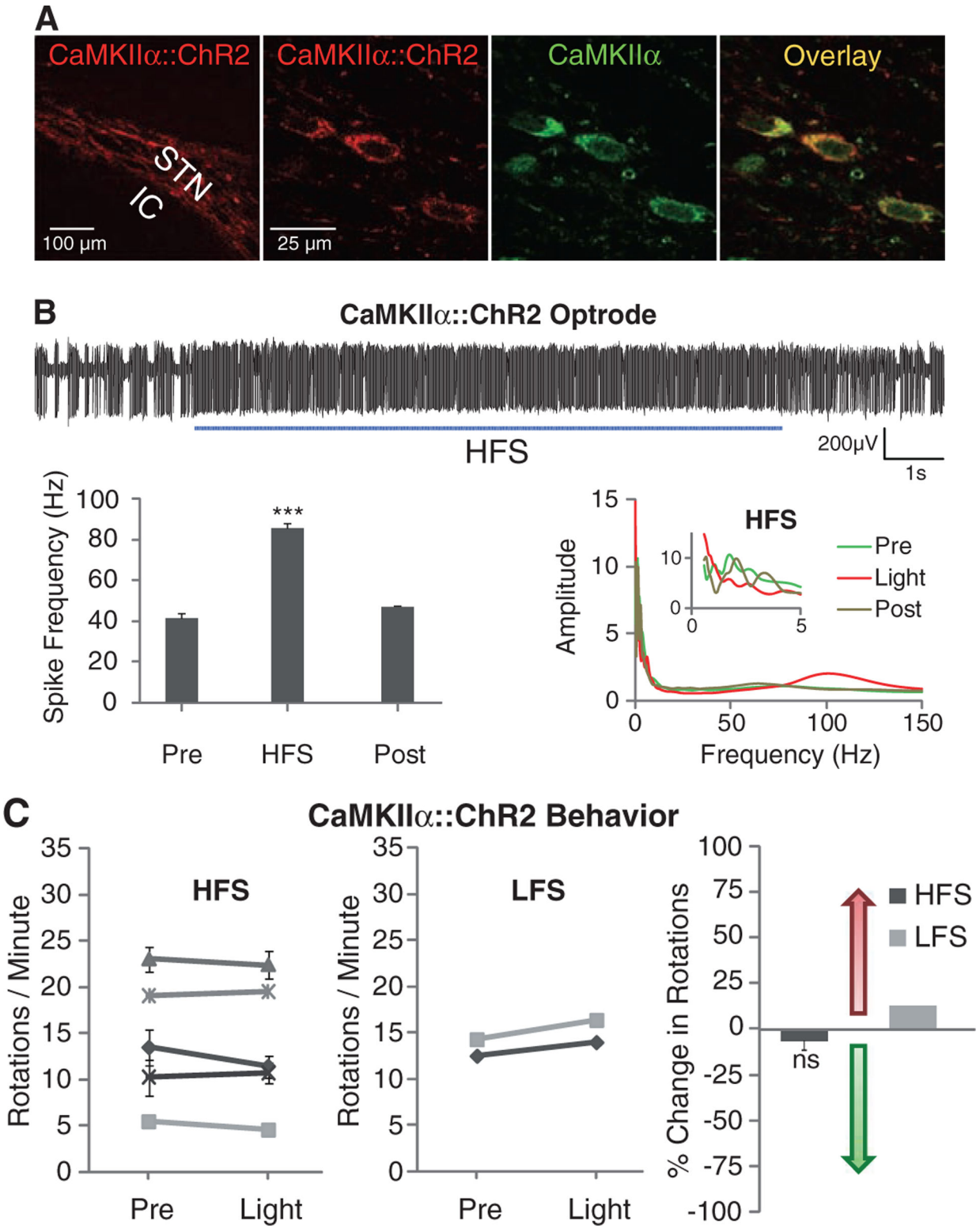

Fig. 3.

Optical depolarization of STN neurons at different frequencies. (**A**) Confocal images of STN neurons expressing CaMKIIα::ChR2-mCherry and labeled for the excitatory neuron–

specific CaMKIIα marker. (**B**) Optical HFS (120 Hz, 5-ms pulse width) of the STN expressing CaMKIIα::ChR2-mCherry in 6-OHDA rats recorded with the optrode connected to a 473-nm laser diode (representative trace and amplitude spectrum shown). Frequency of spiking increased from 41 ± 2 Hz to 85 ± 2 Hz (HFS versus pre, n = five traces: P <0.001, t test, post, n = three traces; traces were sampled from different STN coordinates in one animal). (**C**) Amphetamine-induced rotations were not affected by high (left, 130 Hz, 5-ms pulse width, n = five rats) or low (middle, 20 Hz, 5-ms pulse width, n = two rats) frequency optical stimulation.

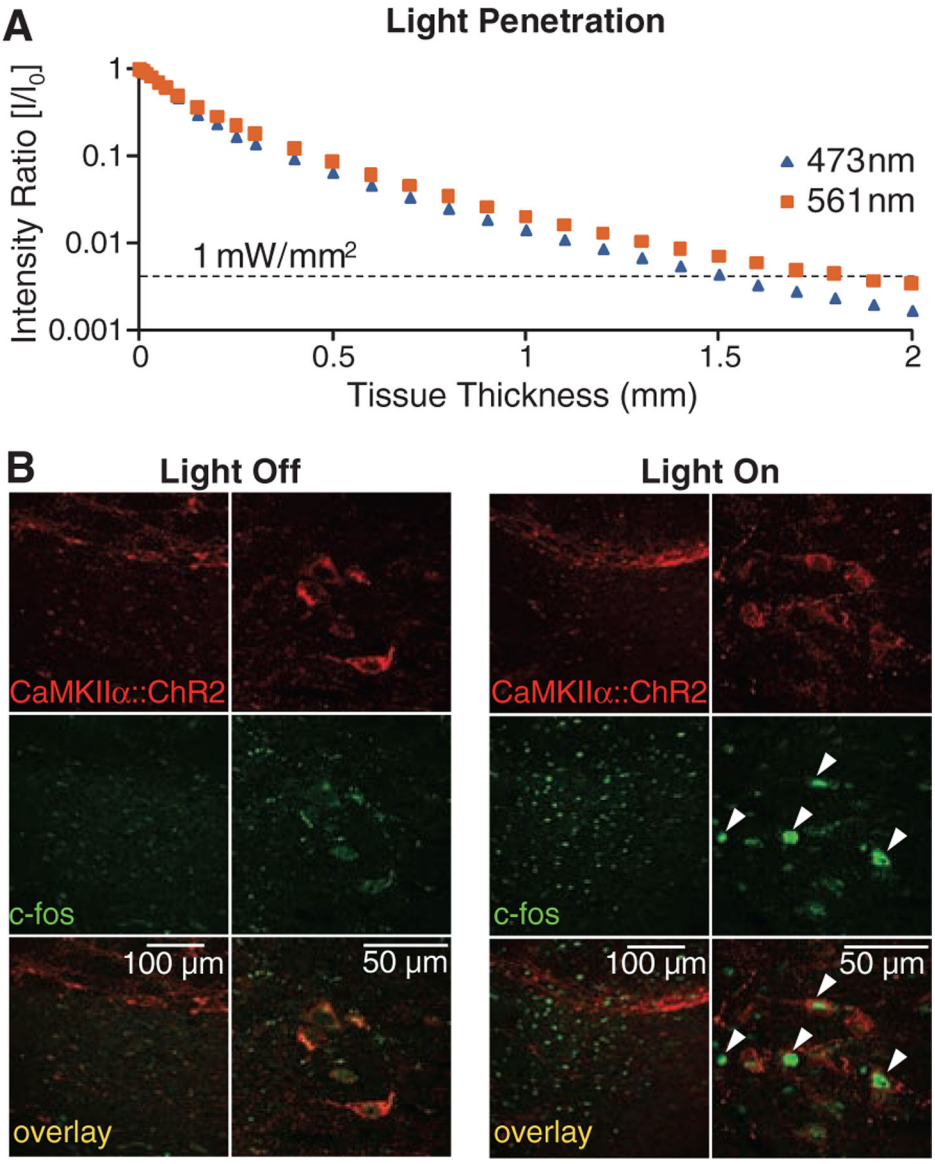

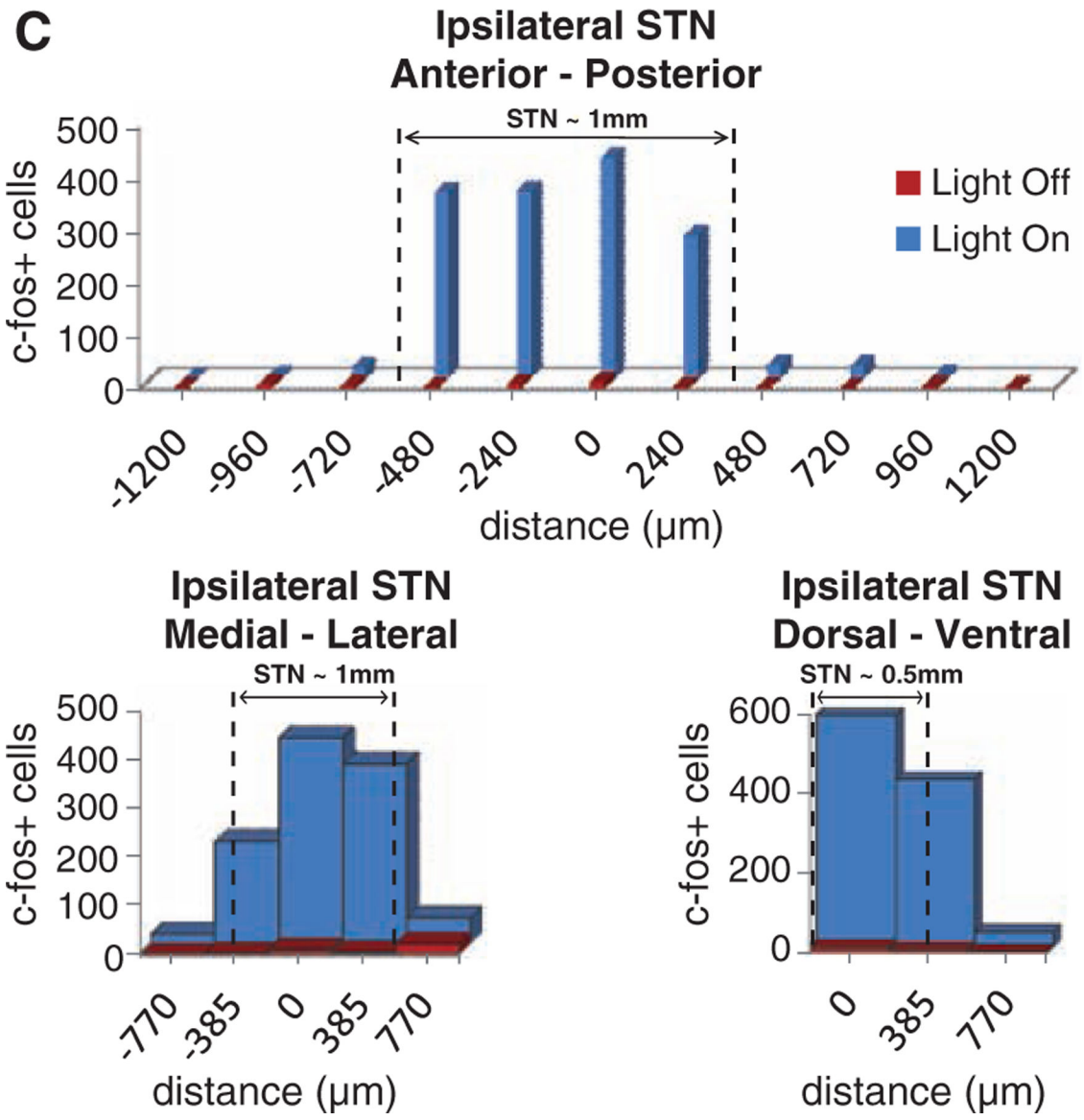

Fig. 4.

Quantification of the tissue volume recruited by optical intervention. (**A**) Intensity values for 473-nm (blue) and 561-nm (yellow) light are shown for a 400-μm fiber as a function of depth in brain tissue. The dashed line at 1 mW/mm^2 (30 mW light source) indicates the minimum intensity required to activate channelrhodopsins and halorhodopsins (16, 20). (**B**) Confocal images of STN neurons expressing CaMKIIα::ChR2-mCherry and labeled for the immediate early gene product c-fos show robust neuronal activation produced by light stimulation in vivo. Arrowheads indicate c-fos–positive cells. Freely moving rats expressing ChR2 in STN (same animals as in Fig. 3), were stimulated with 473-nm light (20 Hz, 5-ms pulse width). (**C**) The STN volume that showed strong c-fos activation was estimated to be at least 0.7 mm^3 (dashed lines indicate STN boundaries); robust c-fos activation was observed medial-lateral (1.155 mm), anterior-posterior (0.800 mm), and dorsal-ventral

(0.770 mm) on subthalamic slices imaged by confocal microscopy with 4′,6′-diamidino-2-phenylindole (DAPI) counterstain.

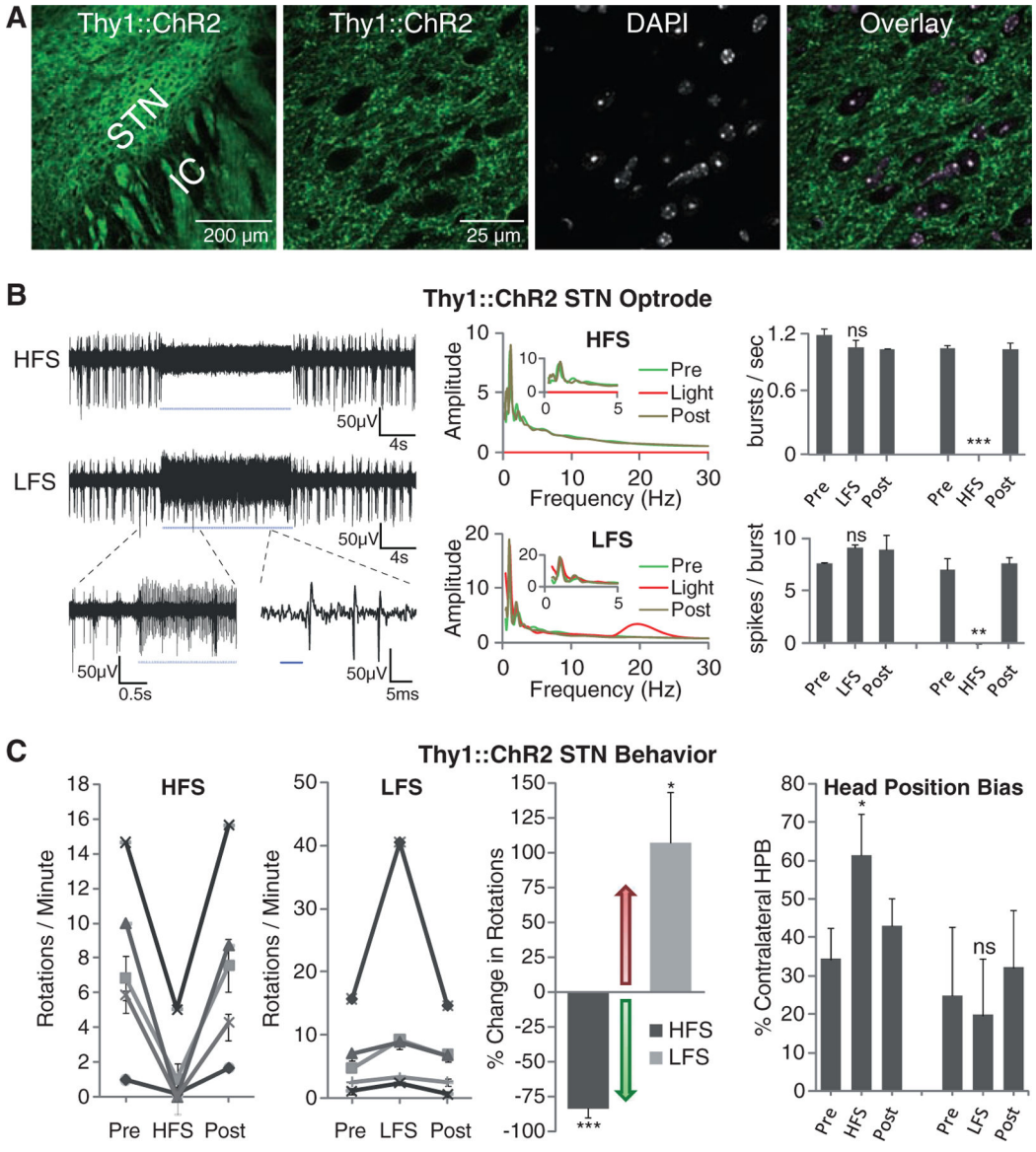

Fig. 5.

Selective optical control of afferent fibers in the STN. (**A**) Confocal images of Thy1::ChR2-EYFP expression in the STN and DAPI staining for nuclei shows selective expression in fibers and not cell bodies (right). (**B**) Optical HFS (130 Hz, 5-ms pulse width) of the STN region in an anesthetized Thy1::ChR2-EYFP 6-OHDA mouse with 473-nm light inhibited STN large-amplitude spikes (sample trace, top left), while inducing smaller-amplitude high-frequency oscillations (figs. S4, C and D, and S5C). Optical LFS (20 Hz, 5-ms pulse width) produced reliable spiking at 20 Hz (bottom left). Whereas HFS prevented bursting (top right, $P < 0.001$, $n = 3$), LFS had no significant effect on burst frequency by two-sample t test ($P > 0.05$, n = three traces) nor on spikes per burst (bottom right, $P > 0.05$, n = three traces). (**C**) Optical HFS to STN in these animals (left, 100 to 130 Hz, 5-ms pulse width, n = five mice) produced robust therapeutic effects, reducing ipsilateral rotations and allowing animals to freely switch directions. In contrast, optical LFS (second left, 20 Hz, 5-ms pulse width, n =

five mice) exacerbated pathologic effects, causing increased ipsilateral rotations. Both effects were reversible (post). Changes were significant by *t* test with μ = 0 for both HFS ($P < 0.001$, n = five mice) and LFS ($P < 0.05$, n = five mice) compared with baseline (light off). (Right) Contralateral head position bias also showed robust correction with HFS by two-sample *t* test (HFS versus light off: $P < 0.05$; n = two mice), but not with LFS (LFS versus light off: $P > 0.05$, n = two mice).

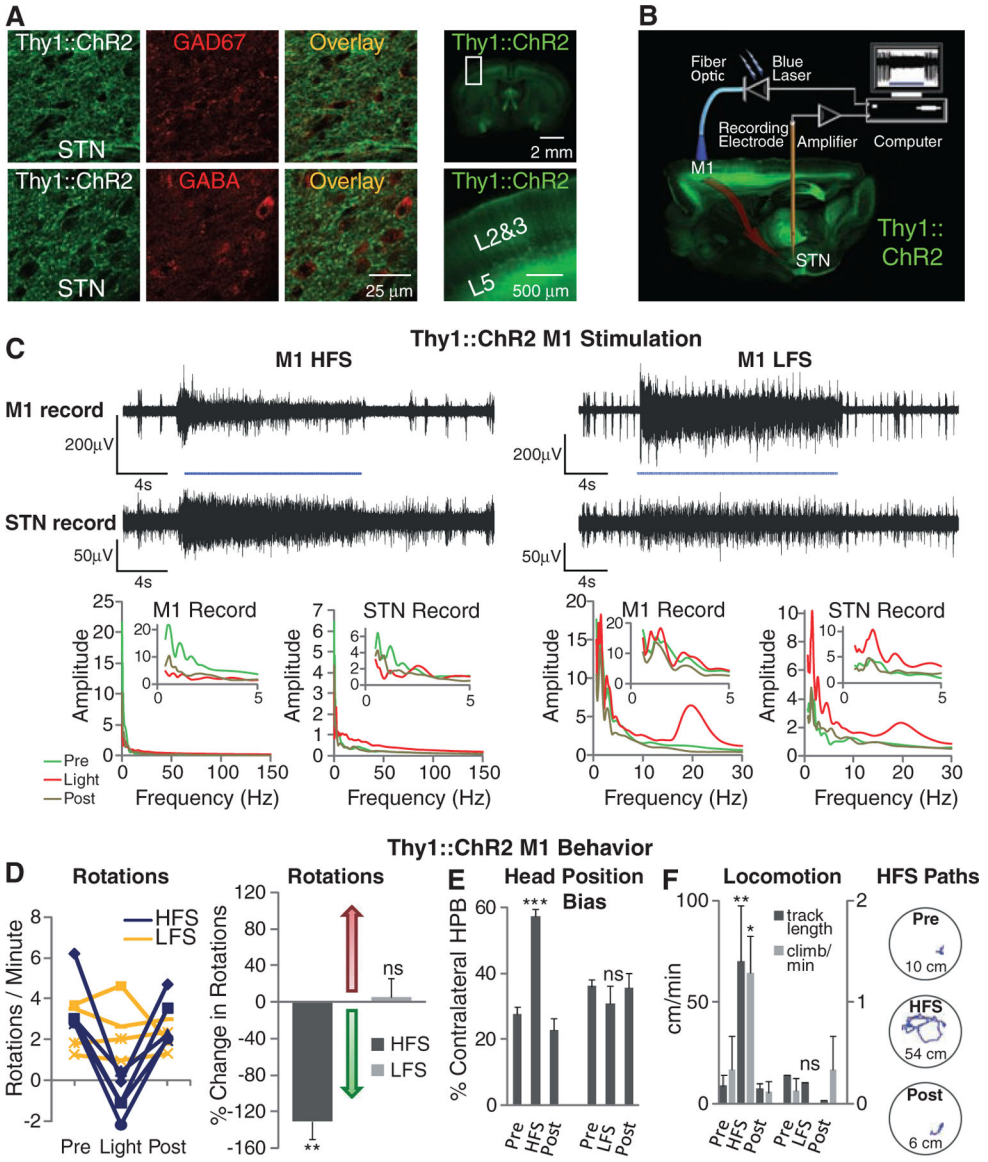

Fig. 6.

Selective optical stimulation of layer V neurons in anterior primary motor cortex. (**A**) GAD67 and GABA staining showed no colocalization with Thy1::ChR2-EYFP in STN (left). Apical dendrites of layer V neurons can be seen rising to the pial surface (22, 23) (right). (**B**) Schematic for optical stimulation of M1 with simultaneous recording in STN of Thy1::ChR2 mice. (**C**) Optical stimulation (473 nm) of M1 and simultaneous recording in STN of anesthetized Thy1::ChR2 mice. Optical HFS (130 Hz, 5-ms pulse width) of M1 modulated activity in both M1 and STN. Optical LFS (20 Hz, 5-ms pulse width) of M1 produced 20-Hz tonic firing in both M1 and STN. (**D**) Optical HFS (130 Hz, 5-ms pulse width) reduced amphetamine-induced ipsilateral rotations in 6-OHDA Thy1::ChR2 mice ($P < 0.01$, n = five mice) in contrast to optical LFS (20 Hz, 5-ms pulse width, $P > 0.05$, n = four mice); t test with µ = 0. (**E**) Contralateral head position bias was corrected in HFS (HFS versus light off: $P < 0.001$, n = four mice), whereas LFS had little effect (LFS versus light

off: $P > 0.05$, n = three mice); two-sample t test. (**F**) HFS but not LFS to M1 significantly increased path length (HFS, $P < 0.01$, n = two mice) and climbing ($P < 0.05$, n = three mice); two-sample t test. Sample paths before, during, and after HFS are shown (100 s each, path lengths noted in cm).